

## Article

# Multilevel Gene Regulation Using Switchable Transcription Terminator and Toehold Switch in *Escherichia coli*

Seongho Hong <sup>†</sup>, Jeongwon Kim <sup>†</sup> and Jongmin Kim <sup>\*</sup>

Department of Life Sciences, Pohang University of Sciences and Technology, Pohang 37673, Korea; shhong1205@postech.ac.kr (S.H.); jeongwon96@postech.ac.kr (J.K.)

<sup>\*</sup> Correspondence: jongmin.kim@postech.ac.kr

<sup>†</sup> These authors contributed equally: Seongho Hong, Jeongwon Kim.

**Abstract:** Nucleic acid-based regulatory components provide a promising toolbox for constructing synthetic biological circuits due to their design flexibility and seamless integration towards complex systems. In particular, small-transcriptional activating RNA (STAR) and toehold switch as regulators of transcription and translation steps have shown a large library size and a wide dynamic range, meeting the criteria to scale up genetic circuit construction. Still, there are limited attempts to integrate the heterogeneous regulatory components for multilevel regulatory circuits in living cells. In this work, inspired by the design principle of STAR, we designed several switchable transcription terminators starting from natural and synthetic terminators. These switchable terminators could be designed to respond to specific RNA triggers with minimal sequence constraints. When combined with toehold switches, the switchable terminators allow simultaneous control of transcription and translation processes to minimize leakage in *Escherichia coli*. Further, we demonstrated a set of logic gates implementing 2-input AND circuits and multiplexing capabilities to control two different output proteins. This study shows the potential of novel switchable terminator designs that can be computationally designed and seamlessly integrated with other regulatory components, promising to help scale up the complexity of synthetic gene circuits in living cells.

**Keywords:** riboregulator; switchable terminator (SWT); small-transcriptional activating RNA (STAR); toehold switch (THS); leakage control; 2-input AND gate; multilevel regulation; multiplexing



**Citation:** Hong, S.; Kim, J.; Kim, J. Multilevel Gene Regulation Using Switchable Transcription Terminator and Toehold Switch in *Escherichia coli*. *Appl. Sci.* **2021**, *11*, 4532. <https://doi.org/10.3390/app11104532>

Academic Editors: Michal Sobkowski, Joanna Romanowska and Michal Sobkowski

Received: 31 March 2021

Accepted: 11 May 2021

Published: 16 May 2021

**Publisher's Note:** MDPI stays neutral with regard to jurisdictional claims in published maps and institutional affiliations.



**Copyright:** © 2021 by the authors. Licensee MDPI, Basel, Switzerland. This article is an open access article distributed under the terms and conditions of the Creative Commons Attribution (CC BY) license (<https://creativecommons.org/licenses/by/4.0/>).

## 1. Introduction

Synthetic biology is an emerging discipline that combines the practice of engineering and biological sciences and promises to provide transformative tools for emerging challenges in the future [1,2]. Remarkable progress has been made in the area of synthetic circuit construction in living organisms, including oscillators, logic gates, bistable switches, and arithmetic circuits [3–6]. Researchers could harness a wealth of natural and engineered parts composed of nucleic acids and proteins and demonstrate their composition towards complex functionality in vitro and in vivo [7–10]. The recent progress in synthetic biology will herald novel applications such as biofuel production, biosensor development, and drug synthesis [11–13].

In particular, nucleic acid-based regulatory circuits provide a promising toolbox for constructing synthetic biological systems due to their design flexibility and seamless integration towards more complex systems [14,15]. RNA-based regulators can modulate transcription and translation steps while providing fast response times and reduced usage of precious cellular resources [1,16,17]. Since the speed of signal propagation in a network is governed by the decay rate of the signal [18], RNA signaling networks have the potential to operate on time scales faster than proteins. On average, the half-life of RNA in the bacterial system is on the order of a few minutes, which is as short as one-hundredth of that of stable proteins [19]. Furthermore, the translation step is not required for the RNA-only transcription controller such that ribosome occupancy and amino acid usage can

also be minimized. In addition, RNA regulatory components require much less encoding space compared to their protein counterparts, which can be crucial to overcoming the limited capacity for carrying genetic programs in a single cell [20]. Together with a deeper understanding of RNA biology [21] and the development of computational tools [22,23], synthetic RNA regulators are poised to accelerate the advancement in synthetic biology [24].

With the growing interest in using RNA to build synthetic control devices, several successful examples of synthetic RNA-based regulatory devices have been reported and could be integrated into more complex genetic circuits [25]. Inspired by natural temperature-sensitive RNA structures, synthetic RNA temperature sensors have been demonstrated that respond to temperature changes through conformational changes of the RNA hairpin structures (Figure 1a) [26]. Temperature-dependent melting of hairpin secondary structure exposes the ribosome binding site (RBS), and protein translation can occur. RNA itself can serve as an input to control RNA devices via Watson-Crick base-pairing rules. For instance, cis-repressor forms base pairing with RBS to occlude translation initiation. The interaction of cis-repressor and trans-acting RNA induces a conformational change of cis-repressor such that the RBS is accessible and protein translation can be initiated (Figure 1b) [16]. Small molecule and protein-responsive RNA control devices have been engineered by coupling aptamers to gene regulatory components due to their high affinity and specificity to target molecules [27,28]. For example, an aptazyme, combining a theophylline RNA aptamer to a hammerhead ribozyme, represses downstream gene expression by sequestering RBS within the ribozyme stem (Figure 1c) [29]. When theophylline is available, the ligand-aptamer interaction induces a conformational change of ribozyme to induce cleavage of its stem, thereby allowing translation of the downstream gene.

De novo-designed synthetic RNA regulators, small-transcriptional activating RNA (STAR) and toehold switch (THS), which each operate at transcription and translation steps, offer promising toolbox with large library size and high dynamic ranges rivalling those of well-known protein regulators [30,31]. For example, a library of 73 TetR-family repressors showed 5- to 207-fold change with up to 16 orthogonal repressor sets [32]. De novo-designed RNA regulators, STAR and THS, demonstrated libraries with comparable dynamic range and orthogonality. STAR system is composed of a target RNA placed upstream of a gene that, once transcribed, folds into a rho-independent transcription terminator, preventing transcription of the downstream gene (Figure S1a) [30]. Upon interaction between target RNA and cognate antisense RNA, the terminator formation is prevented, allowing transcription of the downstream gene. The STAR library was further expanded through computational design [33], applied to plant viral RNA detection [34], and switchable feedback regulators [35]. However, the STAR library was created by randomizing only the upstream linear toehold sequences rather than the stem-loop sequence of terminators; in that sense, the design flexibility of the STAR system remains underexplored. On the other hand, THS is a riboregulator that regulates gene expression at the translation stage (Figure S1b). THS demonstrated high ON/OFF ratios and straightforward concatenation and expansion towards complex logic evaluation; however, some leaky expressions were observed even in the absence of trigger RNA, possibly due to the presence of complete RBS within THS RNA [31,36]. The presence of leaky expression may require further containment in order to construct complex multilayered circuit architecture [37], and consequently, recent studies aimed to demonstrate tight leakage control by simultaneous regulation of transcription and translation steps [38–42].

Here, inspired by STAR library construction, we devise novel switchable transcription terminators (SWT) by modifying natural and synthetic terminators with additional engineered toehold sequences. While the STAR library focused on randomization of the linear toehold region upstream of the fixed terminator sequence, SWT was designed to explore a different set of terminator sequences and also the sequence variants of a given terminator to further expand the sequence space of RNA transcription regulators. Further, by combining the new SWT with well-characterized THS, we demonstrate a multilevel regulatory system at both transcription and translation steps. This multilevel regulator

showed tight leakage control in *E. coli* and could function as 2-input AND logic gates. In addition, SWT and THS can be flexibly combined for controlling multiple fluorescent proteins and could prove useful in multi-layer circuits in vivo. Together, we demonstrated novel RNA-only transcription control elements that can be seamlessly integrated with other RNA regulatory elements, promising to expand the capabilities of RNA synthetic biology.

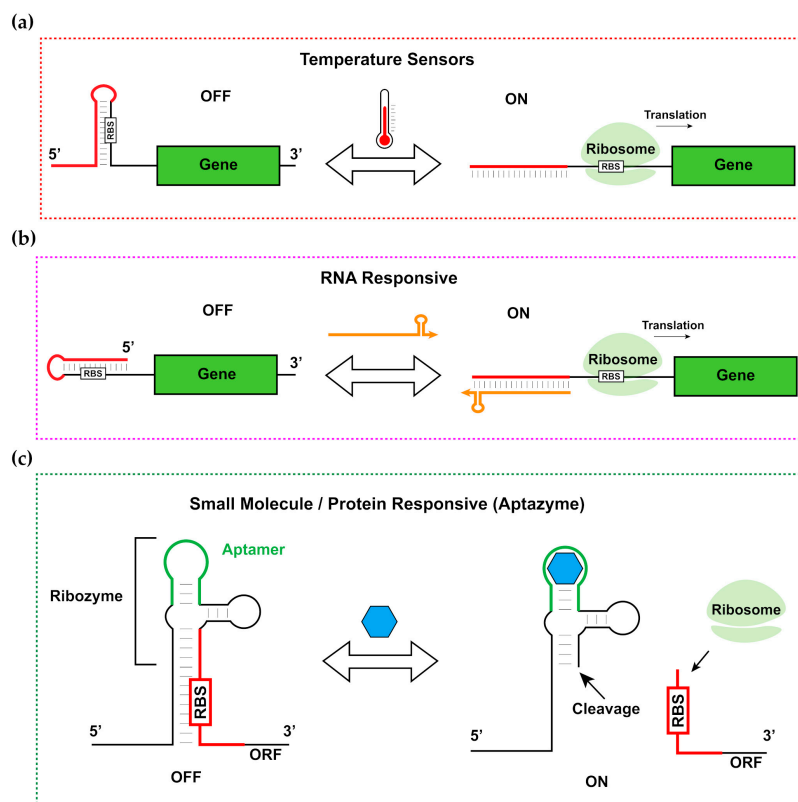


**Figure 1.** Design Strategies for Synthetic RNA Regulators. (a) Schematic of synthetic RNA temperature sensors. When the temperature increases to a certain range, temperature-dependent melting of sensor's stem-loop secondary structure exposes the RBS to initiate translation. (b) Schematic of RNA-responsive RNA devices. The interaction of cis-repressor and trans-acting RNA induces a conformational change of cis-repressor such that the RBS is accessible and protein translation can be initiated. (c) Schematic of small molecule/protein-responsive RNA devices (Aptazyme). The interaction of a specific ligand and its aptamer causes a conformational change, thereby activating a ribozyme to cleave its stem. The released single-stranded RNA can then be translated by the ribosome.

## 2. Materials and Methods

In this section, we describe a shortened version of Materials and Methods. Readers are referred to Detailed Experimental Protocols Section in Supplementary Information for further information.

### 2.1. Plasmid Construction and *E. coli* Strains Used

Backbones for the plasmids were taken from the commercial vectors pET15b, pCOLADuet, pCDFDuet, and pACYCDuet (EMD Millipore, Burlington, MA, USA). SWT, THS, and multilevel regulators were constructed in pCOLADuet. SWT trigger and THS trigger RNAs were constructed in pCDFDuet and pET15b. Additional multilevel regulators for multiplexing experiments were constructed in pACYCDuet. Basic SWT and multilevel regulator constructs were cloned via Gibson assembly. SWT variants construction was done by round-the-horn site-directed mutagenesis using 5'-phosphorylated primers. Plasmid architecture and specific part sequences are listed in Supplementary Information

(Tables S1–S7). Plasmid sequences were confirmed by DNA sequencing. Plasmids were transformed into strains via chemical transformation. *E. coli* BL21 (DE3) strain was used for all in vivo tests.

## 2.2. Media, Chemicals, and Other Reagents

Strains were cultured in LB liquid medium or on LB agar plates (1.5% agar), supplemented with appropriate antibiotics: pCOLADuet (50 µg/mL Kanamycin), pCDFDuet (50 µg/mL Spectinomycin), pET15b (100 µg/mL Ampicillin), pACYCDuet (25 µg/mL Chloramphenicol). M9 media (1× M9 minimal salts, 0.4% glucose, and 2 mM MgSO<sub>4</sub>, 0.1 mM CaCl<sub>2</sub>) was used for flow cytometry analysis; LB liquid media was used for plate-reader analysis of multilayered circuits. IPTG induction was at 1 mM, and anhydrotetracycline (aTc) induction was at 40 ng/mL unless otherwise noted.

## 2.3. Flow Cytometry Analysis

Overnight cultured cells were diluted 1/50-fold, and IPTG was treated immediately. After four hours post IPTG induction, cells were diluted using 1× phosphate-buffered saline (PBS) prior to loading to flow cytometer. The number of replicates was three for each condition. Flow cytometry measurements were performed using a CytoFLEX Flow Cytometer (Beckman Coulter, Pasadena, CA, USA), and at least 15,000 cell events were recorded for each measurement. Acquired data were analyzed using CytExpert software.

## 2.4. Quantitative Reverse-Transcription PCR for Transcription Termination Verification

Culturing and induction of the cells were performed in the same way as the flow cytometry analysis. In DNase/RNase-free condition, total RNA was extracted using RiboEx (GeneAll, Seoul, Korea) reagent. Sample concentration and purity were measured using a BioTek Synergy H1 plate reader (BioTek, Winooski, VT, USA). cDNA was synthesized with 250 ng of total RNA as the template using GFP specific reverse transcription (RT) primer. The cDNA was then used for subsequent analysis in a quantitative PCR step in Stratagene Mx3000P (Agilent Technologies, Santa Clara, CA, USA) with the following conditions: 50 °C for 2 min, 95 °C for 10 min, followed by 40 cycles of 95 °C for 15 s and 60 °C for 1 min. The number of replicates was three for each condition. All of the measurements were followed by melting curve analysis. Ct values were analyzed using MxPRO software (Agilent Technologies, Santa Clara, CA, USA). Primer sequences used in this experiment are listed in Supplementary Information (Table S8).

## 2.5. Plate-Reader Analysis for Multilayered Circuits

Cells were grown overnight and diluted 1/100 fold. After 80 min of recovery, IPTG and aTc were treated, and cells were incubated for an additional 3 h and 30 min. Following the induction, OD600 value and GFP fluorescence (excitation: 479 nm, emission: 520 nm) were measured using BioTek Synergy H1 plate reader. The number of replicates was three for each condition. GFP fluorescence data were normalized by OD600 values (GFP/OD600).

# 3. Results

## 3.1. Switchable Terminator Design

In order to obtain functional terminators amenable to switching, we screened strong rho-independent terminators that satisfy the following characteristics: (a) hairpin loop size as small as 4–5 nt, (b) stem-bottom sequences composed of strong GC pairing, and (c) the stem-loop structure followed by the long poly-U tract [43–46]. We found two candidate terminators satisfying the above design criteria and aimed to modify them with additional engineered toehold domains analogous to the STAR library [30]. As an example, a natural terminator BBa K864600 was selected from the *E. coli* forward terminator library within the iGEM Parts. BBa K864600 showed strong transcription termination strength with an intuitive and short stem-loop structure among the 24 *E. coli* forward terminators (Figure S2) [47,48]. Additionally, a synthetic terminator, T500, was selected due to its very

short hairpin structure and a termination efficiency of close to 98% [45]. T500 terminator has been widely used in synthetic biology applications as an ideal terminator exhibiting a significant elongation complex (EC) dissociation rate [49–51]. Thus, the BBa K864600 and T500 terminators, with their strong transcription termination strengths and short stem-loop structures, can represent ideal targets to be engineered as SWT.

To facilitate hybridization with trigger RNA molecules, we engineered toehold domains upstream of these terminators (Figure 2a and Figure S3). We employed the toehold sequence of STAR target RNA for the SWT and designed cognate trigger RNA such that it can initiate hybridization with SWT at the toehold domain and continue branch migration to disrupt the terminator stem-loop formation. In the absence of trigger RNA, the SWT inhibits downstream gene expression through a rho-independent termination mechanism; however, in the presence of trigger RNA, the RNA–RNA interaction between SWT and cognate trigger RNA disrupts the terminator hairpin formation, allowing transcription of the downstream gene. A functional SWT obtained via modifying the T500 terminator showed a very low leakage level close to that of autofluorescence while allowing strong GFP expression in its ON state (Figure 2b).

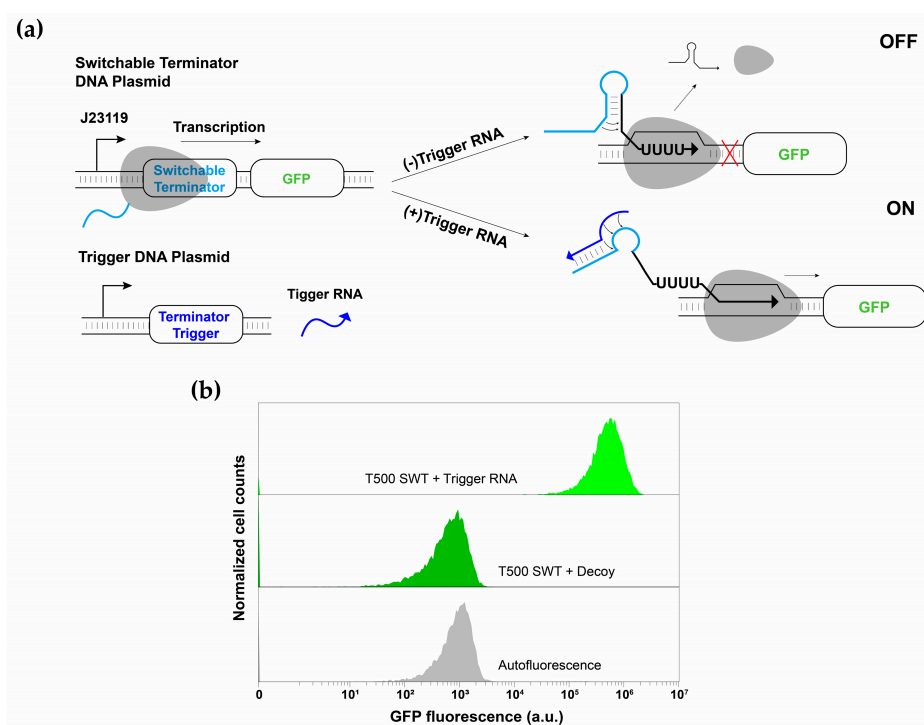


**Figure 2.** Design Schematics of Switchable Terminator (SWT) and GFP Fluorescence Histogram. (a) Design schematics of SWT, where transcription terminators are engineered with an additional toehold domain to facilitate interaction with designed trigger RNA molecules. In the absence of a trigger RNA, the rho-independent terminator is formed, preventing further transcription elongation. In the presence of trigger RNA, the trigger RNA initiates hybridization with SWT at the toehold domain (a–a\*) and continues branch migration to unwind the stem-loop structure of SWT, allowing transcription elongation via RNAP. (b) Flow cytometry GFP fluorescence histograms for SWT based on T500 synthetic terminator in the presence of cognate trigger RNA or decoy RNA. Autofluorescence level was measured from cells not bearing a GFP-expressing plasmid.



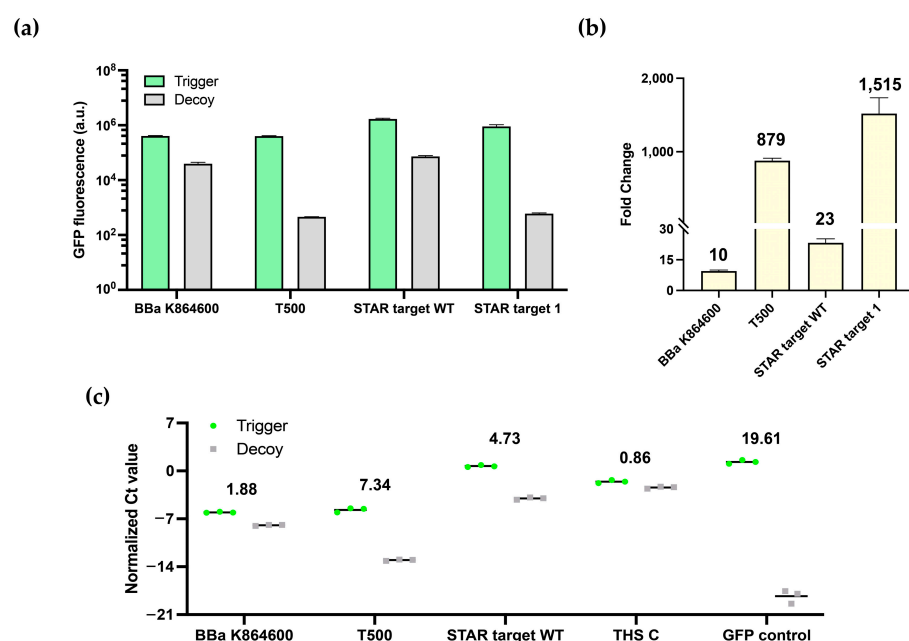


**Figure 3.** In Vivo Characterization of SWT Candidates. (a) Transcription terminators T500 and BBa K864600 were engineered to be responsive to trigger RNA, and these were characterized in vivo. STAR target WT and STAR target 1 were included to benchmark performance. The GFP fluorescence of SWT candidates was measured in the presence of trigger RNA or decoy RNA. Fluorescence levels were expressed on a logarithmic scale. (b) ON/OFF ratios of SWT candidates and STARs were calculated. T500 SWT showed a high-fold change value of 879-fold with low OFF-state fluorescence. Relative errors for the GFP fluorescence are from the s.d. of three biological replicates. (c) Quantitative reverse-transcription PCR results targeting GFP mRNA for SWT candidates and STAR target WT. THS C was used as a control. Ct values were normalized by subtracting the Ct values of 16S rRNA for each sample, and the number above each column indicates the gap between Ct values in the presence of trigger RNA and decoy RNA.

### 3.2. Characterization of Switchable Terminators

To benchmark the regulatory performance of designed SWT, we chose reference constructs among STAR and THS libraries. For STAR, STAR AD1 (STAR target WT) and the best STAR in the computationally designed library (STAR target 1) were selected [30,33]. For THS, three switch-trigger pairs were chosen based on their high fold-change values reported: ACTS\_TypeII\_N1 (THS A), ACTS\_TypeII\_N7 (THS B), and ACTS\_TypeII\_N3 (THS C) [36]. The SWT candidates were tested in *E. coli* BL21 (DE3) strain with the SWT and trigger RNAs expressed from separate medium and high copy plasmids, respectively (Figure 3a). Expression of trigger RNA was induced using IPTG, which initiated the production of SWT trigger RNAs through T7 RNA polymerase. GFP was used to characterize switch output performance via flow cytometry. The BBa K864600 SWT showed a fold change of about 10 and some noticeable leakage levels comparable to the STAR target WT (Figure 3b). On the other hand, the T500 SWT exhibited a nearly 900-fold change with a very low leakage level, providing similar performance to the best STAR reported (STAR target 1).

To test whether the ON/OFF regulation of the SWT is due to the transcription regulation, we performed quantitative reverse-transcription PCR and determined the level of GFP mRNA in the presence and absence of trigger RNA (Figure 3c). As a control, THS C was used, which is regulated at the translational level rather than the transcriptional level [36]. We observed that the Ct values normalized with the conventional reference gene (16S rRNA) corresponded to high and low amounts of GFP mRNA for ON and OFF state of the SWT as expected. Of note, the T500 SWT showed the minimum amount of RNA in the OFF state when compared to BBa K864600 and STAR target WT while maintaining a

large Ct value difference of 7.34 cycles for the ON and OFF states. For RT-qPCR results on the reference gene, 16S rRNA, we observed that there was a very small difference in raw Ct values (typically less than 0.2 cycles) in the presence and absence of cognate trigger RNAs (Table S9). This suggests that the Ct value differences in Figure 3c could reflect the changes in the absolute amount of target GFP mRNA. For T500 SWT, this translates to about a 160-fold difference in the amount of target GFP mRNA, somewhat less than the fold change in GFP fluorescence observed. Thus, the T500 SWT represents a new transcriptional regulator with excellent dynamic features, and therefore, we further characterize and expand T500 SWT through subsequent experiments.

Next, we aimed to investigate the design flexibility of T500 SWT by modifying the critical stem-loop sequence and asked whether it maintains its characteristics as an SWT (Figure 4a). We changed 3 base pairs at the bottom of the hairpin, which is considered critical to the terminator function [43]. Positions were named P1, P2, and P3 starting from the bottom of the stem, and the base compositions were adjusted by swapping G and C bases (V1), changing to G-U wobble base pair (V2), and changing to A-U base pair (V3). Three sequence variants were generated for the bottom of the stem, while G-C to A-U changes were also implemented in the other positions, and the resulting GFP fluorescence changes were measured in vivo (Figure 4b,c). Interestingly, the OFF-state GFP fluorescence level was similar to that of T500 original SWT for all sequence variants. However, the ON-state GFP expression levels were reduced for these sequence variants for reasons that are not clear (Figure 4d). Still, we confirmed that certain sequence modifications within the critical terminator hairpin sequence of the T500 SWT could be tolerated, suggesting that further sequence optimization should be possible.

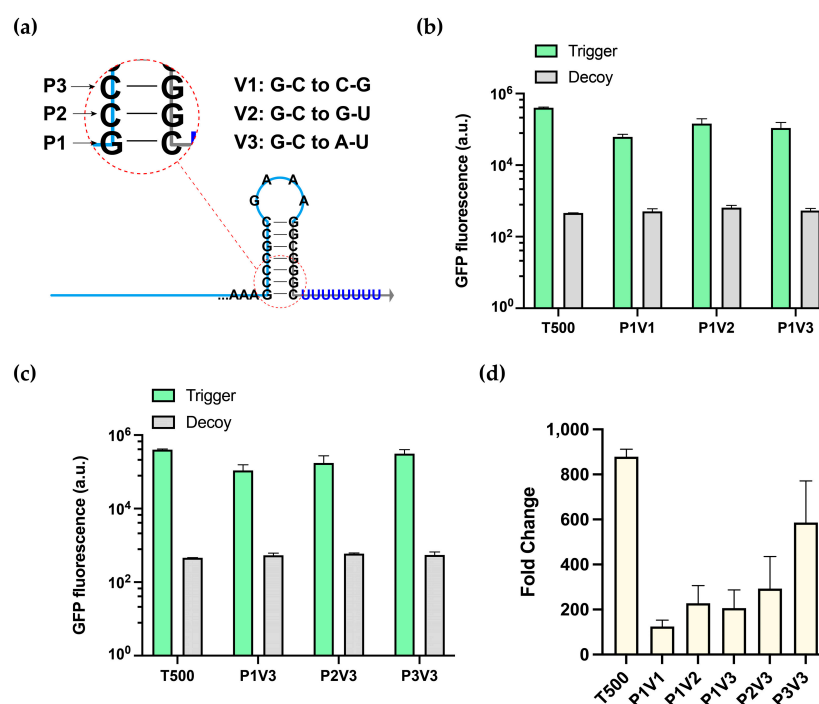


**Figure 4.** Design and Characterization of T500 SWT Variants. (a) Schematic of the stem sequence variants of T500 SWT. The positions and types of mutation are indicated by P and V. (b) The GFP fluorescence of T500 SWT sequence variants at P1 was measured in the presence of trigger RNA or decoy RNA. Fluorescence levels were expressed on a logarithmic scale. (c) The GFP fluorescence of T500 SWT sequence variants (V3: G-C to A-U) was measured in the presence of trigger RNA or decoy RNA. Fluorescence levels were expressed on a logarithmic scale. (d) ON/OFF ratios for T500 SWT sequence variants were calculated. Relative errors for the GFP fluorescence are from the s.d. of three biological replicates.

### 3.3. Multilevel Regulatory System and 2-Input AND-Gate Implementation

Building on the success of T500 SWT as a transcriptional regulator, we designed a multilevel regulator that simultaneously controls transcription and translation by concatenating the T500 SWT with the well-characterized translational regulator THS. The SWT should be turned on by the cognate SWT trigger RNA to allow transcription of the downstream THS connected to the target gene (Figure 5a). In the absence of the THS trigger RNA, the RBS remains enclosed within the stem-loop of THS, preventing the ribosome access and translation of the target gene [31]. If cognate THS trigger RNA is also present, the hairpin structure of THS could be unwound by the trigger RNA, exposing RBS and start codon to activate translation of the downstream gene (Figure 5b). Note that this multilevel regulatory system is essentially functioning as a 2-input AND gate where the target gene is expressed only when both SWT trigger RNA and THS trigger RNA are present (Figure 5c). Since target gene expression is regulated both at transcription and translation levels, tighter expression control may be achieved when compared to regulation at a single stage.

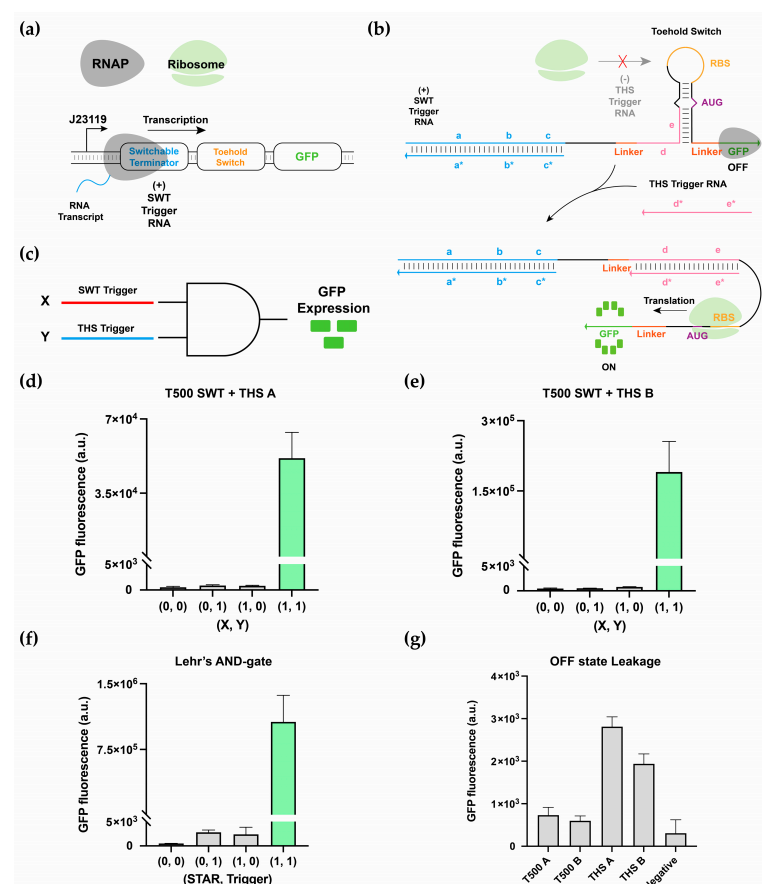


**Figure 5.** Implementation of 2-input AND Gates via Multilevel Regulatory System. (a,b) Design schematics of a multilevel regulatory system that concatenates SWT and THS in the same expression cassette. Transcription is controlled by SWT trigger RNA (a), and the subsequent translation of the downstream gene is controlled by THS trigger RNA (b). Thus, the output gene expression can occur only in the presence of both SWT and THS trigger RNAs. (c) Schematic of the 2-input AND gate formed by the multilevel regulator. (d–f) The truth table for the AND computations: T500 SWT + THS A (d), T500 SWT + THS B (e), and an analogous construct previously reported [38] (f). The multilevel regulators that combine T500 SWT and THS showed very low leakage levels for (0, 1) and (1, 0) input combinations in contrast to the previous regulator shown in (f). (g) The OFF states were compared for multilevel regulatory circuits and the constituent single THS. The negative control contained an empty pCOLADuet plasmid. Relative errors for the GFP fluorescence are from the s.d. of three biological replicates.



We created multilevel regulatory systems by connecting the T500 SWT with THS A (T500 A) and THS B (T500 B) from the second generation THS library [36]. For both multilevel regulators, the GFP expression patterns were consistent with the 2-input logical AND gate with SWT and THS triggers as inputs (Figure 5d,e). The multilevel regulators demonstrated very low GFP expression in all three logical FALSE conditions and strong GFP expression in the sole logical TRUE condition. To benchmark the performance of our multilevel regulators, we also tested a previously reported 2-input AND gate connecting the STAR target RNA and the first generation THS in the same transcript (Figure 5f) [38]. Notably, the leakage levels of our designs were lower than the OFF state of Lehr's AND-gate (Figures S4 and S5). Additionally, the leakage level of multilevel regulators was much lower than those of constituent THS (Figure 5g), suggesting the improved leakage control and logic capability of SWT and THS combinations.

### 3.4. Multiplexing of 2-Input AND-Gates

To further demonstrate multiplexing capabilities, we designed a system where each multilevel regulator (T500 A and the T500 B) controls a different fluorescent reporter protein (GFP and mCherry), resulting in a 3-input and 2-output circuitry (Figure 6a). We expressed these two multilevel regulators in the same cell and evaluated their performance for the 8-element truth table consisting of all three input combinations (Figure 6b). GFP expression was regulated by SWT and THS A triggers, and mCherry expression was regulated by SWT and THS B triggers as expected with no apparent crosstalk. With all three triggers present, the mCherry expression level was slightly decreased as compared to when mCherry was expressed alone, possibly due to increased cellular burden to express both reporter proteins at the same time. The multiplexing circuits can also be successfully implemented for different regulator-reporter combinations (Figure S6), suggesting its potential as a route to scale up the complexity of multiplexing circuits.

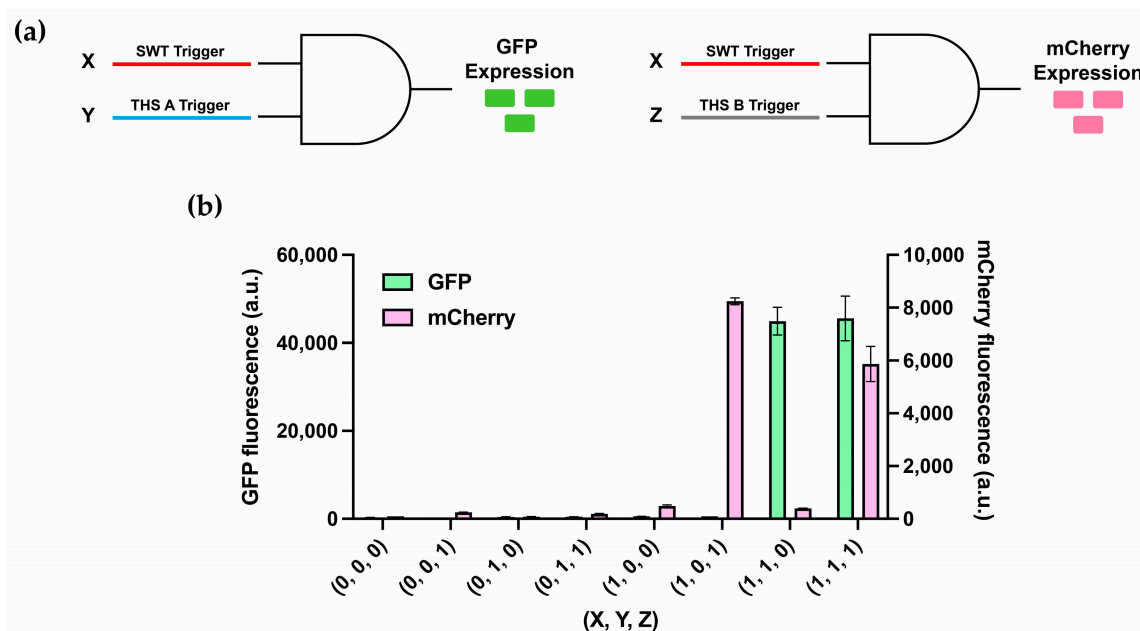


**Figure 6.** Multiplexed Gene Expression Control by Multilevel Regulatory Systems. (a) Design schematics of multiplexing implementation. GFP is expressed under the control of the T500 SWT trigger and THS A trigger, and mCherry is expressed under the control of the T500 SWT trigger and THS B trigger. (b) Measurement of fluorescent protein outputs via flow cytometry for all input combinations. Each reporter protein was expressed in the presence of an appropriate combination of cognate triggers as expected. Relative errors for GFP and mCherry fluorescence are from the s.d. of three biological replicates.

### 3.5. Multilayered Circuit Construction Using SWT

To further characterize the applicability of SWT as a versatile synthetic regulator, we constructed a multilayered circuit with SWT as the top regulator. In this design, T500 SWT regulates the expression of TetR in the first layer, which in turn regulates GFP reporter expression in the second layer (Figure 7a). Since transcription of GFP reporter from T7 promoter can be strongly inhibited by TetR binding to its operator site (TetO), any leaky expression of TetR from the first layer can strongly inhibit the GFP reporter expression (Figure 7b and Figure S7) [52,53]. When TetR was under the control of STAR Target AD1 or THS in the first layer, GFP reporter expression was repressed by leaky TetR even in the absence of cognate trigger RNA. GFP expression levels could be partially restored when anhydrotetracycline (aTc) was treated, indicating that TetR was, in fact, inhibiting GFP expression in the second layer. However, when the T500 SWT was connected to TetR in the first layer, the GFP repression by leaky TetR was not observed despite the fact that a strong constitutive promoter J23119 was driving the expression of T500 SWT-TetR (Figure 7c) [54]. In the presence of cognate trigger RNA, T500 SWT-TetR could strongly repress GFP reporter expression (Figure 7d), indicating proper expression of TetR in its ON state. Even in the presence of cognate trigger RNA, GFP expression levels were recovered to some extent when higher aTc levels were used (Figure S8). Together, SWT design can be utilized in multilayered complex circuits thanks to its extremely low leakage and large dynamic range.

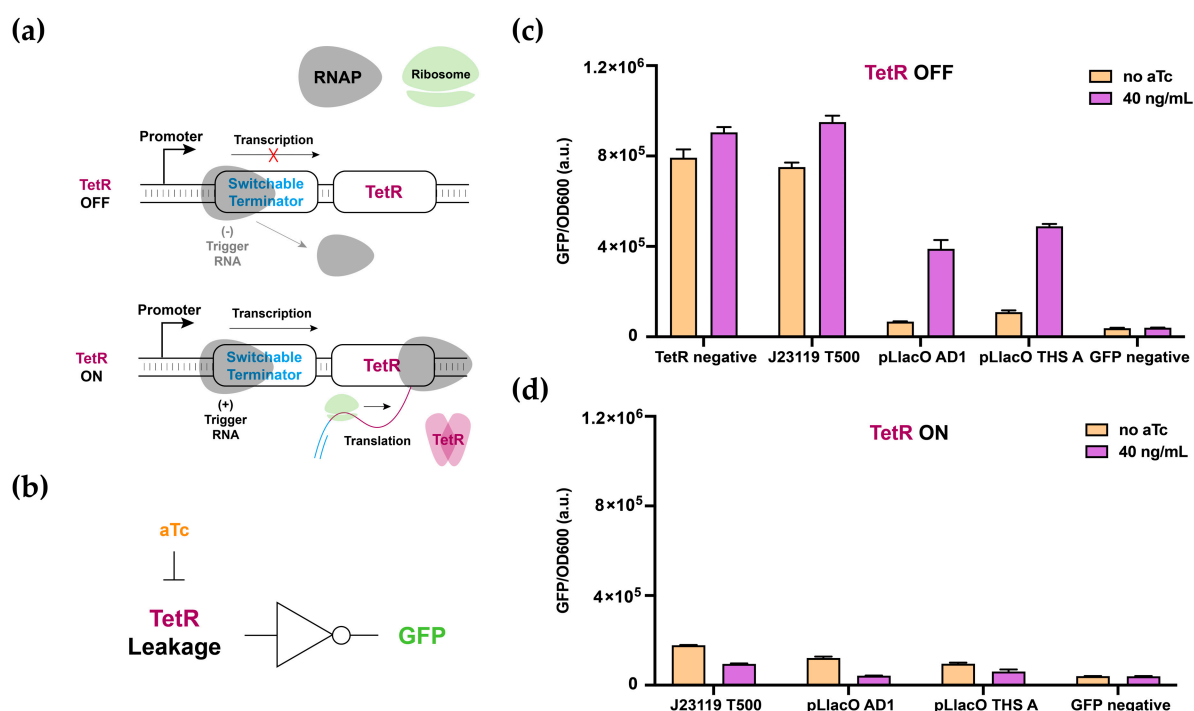


**Figure 7.** Characterization of Multilayered Circuits. (a) Design of circuits where TetR is under the control of SWT. (b) Simplified schematic of SWT-TetR and pT7 (TetO)-GFP multilayered circuit. This multilayered circuit is analogous to a NOT logic gate where TetR expression from the first layer suppresses the expression of GFP reporter output in the next layer (see Figure S7 for details). In case there is a leaky TetR expression, GFP output would be suppressed even in the absence of trigger RNA, which can be partly reversed by aTc treatment. (c,d) T500 SWT, STAR target WT, or THS A was attached upstream of TetR to regulate its expression. GFP fluorescence outputs were measured in the absence of trigger RNA (c) and in the presence of trigger RNA (d). TetR negative did not contain RBS upstream of the TetR gene, and GFP negative did not contain RBS upstream of the GFP gene. Relative errors for GFP fluorescence are from the s.d. of three biological replicates.

#### 4. Discussion

In this study, we report the design and construction of a novel synthetic transcriptional regulator, SWT, whose transcriptional state is regulated in a switch-like manner by the presence of a cognate RNA trigger. Both natural and synthetic terminators could be converted to SWT by engineering additional toehold domains upstream of the rho-independent terminator sequences. Our best SWT, T500 SWT, showed an extremely low level of leakage and a dynamic range close to the best STAR regulator reported, demonstrating its potential as a promising gene regulatory part. We combined the SWT with THS to create 2-input AND logic gates capable of multilevel regulation both at transcription and translation stages; this multilevel regulator showed leakage levels down to cellular autofluorescence for all logical FALSE states. Further, these multilevel regulators can be easily multiplexed to form 3-input/2-output logic circuits. To test the generality of our design approach, we constructed a multilayered circuit with a TetR repressor under the control of T500 SWT in the first layer and a GFP reporter under the control of TetR in the second layer. We confirmed that the tight leakage control through T500 SWT allowed constructing a functional 2-layer circuit, an improvement over THS and early STAR regulator. Thus, we provide evidence that the SWT can serve as novel transcriptional regulatory elements with desirable dynamics and very low leakage and may find its use in complex synthetic circuits.

Among the SWT designs we tested, the best T500 SWT showed tight leakage control comparable to the best STAR regulator reported while demonstrating much less leaky expression as compared to THS elements; however, the expression level in its ON state was lower than other STAR and THS regulators. To further improve expression levels, a number of sequence optimization strategies can be applied to SWT. For the current version of T500 SWT, we combined the toehold binding domain of the best STAR regulator (STAR Target 1) and RBS sequence from the THS library [30,31]. Higher expression levels may be achieved if the sequence contexts of multiple components such as RBS, linker sequences, and toehold domains of SWT are adjusted at the same time for optimal sequence combination. For instance, we also tested two other toehold sequences from the STAR library [33] for T500 SWT and observed that the ON-state expression level was changed while maintaining the same low leakage level in the OFF state (Figure S3). Therefore, it seems likely that the ON-state can be further optimized without disrupting the tight leakage control of SWT. In case a tighter leakage control is desired, alternative approaches to further reduce leakage level may include elongating the terminator stem and engineering the terminator stem to partially sequester RBS [42]. The design flexibility of RNA structures will likely lead to new developments to circumvent these current limitations.

Our experiments demonstrated SWT as switchable control elements for transcriptional regulation that can complement STAR transcription regulators and enrich the toolbox of RNA synthetic biology [55]. Due to the working mechanism that terminates transcription of the downstream gene in its off state, the resource burden on the host organisms is minimized while achieving tight leakage control. In a multilayered circuit architecture, a low level of input noise can be quickly amplified, requiring much better control of leaky expression at each regulatory level; SWT can provide the tight regulatory control that meets the stringent requirement of multilayered circuits. In addition, these properties of SWT would be effective at managing the production of toxic molecules and could find use in the development of biocontainment technology [56–58]. Taken together, SWT, as a new set of modular transcriptional regulatory components, could provide a much-needed toolkit to build complex synthetic circuits and accelerate advancement in RNA synthetic biology [59].

**Supplementary Materials:** The following are available online at <https://www.mdpi.com/article/10.3390/app11104532/s1>, Detailed Experimental Protocols, Table S1: Plasmids Used in This Study, Table S2: Examples of DNA Plasmid Sequences, Table S3: Promoter Sequences Used in This Study, Table S4: Insert Sequences Used in This Study, Table S5: Trigger Sequences Used in This Study, Table S6: Terminator Sequences Used in This Study, Table S7: Other Accessory Sequences Used in

This Study, Table S8: Primers Used for Reverse Transcription and qPCR, Table S9: RT-qPCR Raw Data, Figure S1: De-novo-designed Synthetic RNA Regulators, STAR and THS, Figure S2: Switchable Terminator Structure and Sequences, Figure S3: Fluorescence Characterization of T500 SWT Toehold Variants, Figure S4: GFP Fluorescence Histograms of Multilevel Regulatory Systems and Single THS, Figure S5: Logical FALSE States of Multilevel Regulatory Systems, Figure S6: Multiplexed Gene Expression Control with Exchanged Reporter Protein, Figure S7: Detailed Schematics of Multilayered Circuits, Figure S8: Characterization of Multilayered Circuits at High aTc Concentrations.

**Author Contributions:** Conceptualization: S.H., J.K. (Jeongwon Kim), and J.K. (Jongmin Kim); Methodology: S.H. and J.K. (Jeongwon Kim); Formal analysis: S.H. and J.K. (Jeongwon Kim); Data curation: S.H. and J.K. (Jeongwon Kim); Supervision: J.K. (Jongmin Kim); Writing—original draft preparation: J.K. (Jeongwon Kim); Writing—review and editing: S.H. and J.K. (Jongmin Kim). All authors have read and agreed to the published version of the manuscript.

**Funding:** This research was supported by the National Research Foundation of Korea (NRF-2019R1A2C1086830) grant funded by the Korean government (MSIT).

**Institutional Review Board Statement:** Not applicable.

**Informed Consent Statement:** Not applicable.

**Data Availability Statement:** The data presented in this study are available on request from the corresponding author.

**Acknowledgments:** We would like to thank Jeongwook Lee for providing us with the necessary equipment for flow cytometry analysis.

**Conflicts of Interest:** The authors declare no conflict of interest.

## References

1. Cameron, D.E.; Bashor, C.J.; Collins, J.J. A brief history of synthetic biology. *Nat. Rev. Microbiol.* **2014**, *12*, 381–390. [\[CrossRef\]](#)
2. Cheng, A.A.; Lu, T.K. Synthetic biology: An emerging engineering discipline. *Annu. Rev. Biomed. Eng.* **2012**, *14*, 155–178. [\[CrossRef\]](#)
3. Elowitz, M.B.; Leibler, S. A synthetic oscillatory network of transcriptional regulators. *Nature* **2000**, *403*, 335–338. [\[CrossRef\]](#) [\[PubMed\]](#)
4. Win, M.N.; Smolke, C.D. Higher-order cellular information processing with synthetic RNA devices. *Science* **2008**, *322*, 456–460. [\[CrossRef\]](#) [\[PubMed\]](#)
5. Kim, J.; White, K.S.; Winfree, E. Construction of an in vitro bistable circuit from synthetic transcriptional switches. *Mol. Syst. Biol.* **2006**, *2*, 68. [\[CrossRef\]](#) [\[PubMed\]](#)
6. Xu, S.; Li, H.; Miao, Y.; Liu, Y.; Wang, E. Implementation of half adder and half subtractor with a simple and universal DNA-based platform. *NPG Asia Mater.* **2013**, *5*, e76. [\[CrossRef\]](#)
7. Sun, Z.Z.; Yeung, E.; Hayes, C.A.; Noireaux, V.; Murray, R.M. Linear DNA for rapid prototyping of synthetic biological circuits in an Escherichia coli based TX-TL cell-free system. *ACS Synth. Biol.* **2014**, *3*, 387–397. [\[CrossRef\]](#)
8. Grünberg, R.; Serrano, L. Strategies for protein synthetic biology. *Nucleic Acids Res.* **2010**, *38*, 2663–2675. [\[CrossRef\]](#)
9. Davidson, E.A.; Ellington, A.D. Synthetic RNA circuits. *Nat. Chem. Biol.* **2007**, *3*, 23–28. [\[CrossRef\]](#)
10. Nielsen, A.A.; Segall-Shapiro, T.H.; Voigt, C.A. Advances in genetic circuit design: Novel biochemistries, deep part mining, and precision gene expression. *Curr. Opin. Chem. Biol.* **2013**, *17*, 878–892. [\[CrossRef\]](#)
11. Jagadevan, S.; Banerjee, A.; Banerjee, C.; Guria, C.; Tiwari, R.; Baweja, M.; Shukla, P. Recent developments in synthetic biology and metabolic engineering in microalgae towards biofuel production. *Biotechnol. Biofuels* **2018**, *11*, 185. [\[CrossRef\]](#) [\[PubMed\]](#)
12. Bereza-Malcolm, L.T.; Mann, G.I.; Franks, A.E. Environmental sensing of heavy metals through whole cell microbial biosensors: A synthetic biology approach. *ACS Synth. Biol.* **2015**, *4*, 535–546. [\[CrossRef\]](#) [\[PubMed\]](#)
13. Trosset, J.-Y.; Carbonell, P. Synthetic biology for pharmaceutical drug discovery. *Drug Des. Dev. Ther.* **2015**, *9*, 6285–6302. [\[CrossRef\]](#) [\[PubMed\]](#)
14. Zhang, D.Y.; Turberfield, A.J.; Yurke, B.; Winfree, E. Engineering entropy-driven reactions and networks catalyzed by DNA. *Science* **2007**, *318*, 1121–1125. [\[CrossRef\]](#)
15. Lee, J.; Kladwang, W.; Lee, M.; Cantu, D.; Azizyan, M.; Kim, H.; Limpacher, A.; Gaikwad, S.; Yoon, S.; Treuille, A. RNA design rules from a massive open laboratory. *Proc. Natl. Acad. Sci. USA* **2014**, *111*, 2122–2127. [\[CrossRef\]](#)
16. Isaacs, F.J.; Dwyer, D.J.; Ding, C.; Pervouchine, D.D.; Cantor, C.R.; Collins, J.J. Engineered riboregulators enable post-transcriptional control of gene expression. *Nat. Biotechnol.* **2004**, *22*, 841–847. [\[CrossRef\]](#)
17. Rodrigo, G.; Landrain, T.E.; Jaramillo, A. De novo automated design of small RNA circuits for engineering synthetic riboregulation in living cells. *Proc. Natl. Acad. Sci. USA* **2012**, *109*, 15271–15276. [\[CrossRef\]](#)
18. Rosenfeld, N.; Alon, U. Response delays and the structure of transcription networks. *J. Mol. Biol.* **2003**, *329*, 645–654. [\[CrossRef\]](#)

19. Laalami, S.; Zig, L.; Putzer, H. Initiation of mRNA decay in bacteria. *Cell. Mol. Life Sci.* **2014**, *71*, 1799–1828. [\[CrossRef\]](#)
20. Na, D.; Yoo, S.M.; Chung, H.; Park, H.; Park, J.H.; Lee, S.Y. Metabolic engineering of Escherichia coli using synthetic small regulatory RNAs. *Nat. Biotechnol.* **2013**, *31*, 170–174. [\[CrossRef\]](#)
21. Qi, L.S.; Arkin, A.P. A versatile framework for microbial engineering using synthetic non-coding RNAs. *Nat. Rev. Microbiol.* **2014**, *12*, 341–354. [\[CrossRef\]](#)
22. Zadeh, J.N.; Steenberg, C.D.; Bois, J.S.; Wolfe, B.R.; Pierce, M.B.; Khan, A.R.; Dirks, R.M.; Pierce, N.A. NUPACK: Analysis and design of nucleic acid systems. *J. Comput. Chem.* **2011**, *32*, 170–173. [\[CrossRef\]](#)
23. Reuter, J.S.; Mathews, D.H. RNAstructure: Software for RNA secondary structure prediction and analysis. *BMC Bioinform.* **2010**, *11*, 129. [\[CrossRef\]](#)
24. Chappell, J.; Watters, K.E.; Takahashi, M.K.; Lucks, J.B. A renaissance in RNA synthetic biology: New mechanisms, applications and tools for the future. *Curr. Opin. Chem. Biol.* **2015**, *28*, 47–56. [\[CrossRef\]](#)
25. Liang, J.C.; Bloom, R.J.; Smolke, C.D. Engineering biological systems with synthetic RNA molecules. *Mol. Cell* **2011**, *43*, 915–926. [\[CrossRef\]](#)
26. Neupert, J.; Karcher, D.; Bock, R. Design of simple synthetic RNA thermometers for temperature-controlled gene expression in Escherichia coli. *Nucleic Acids Res.* **2008**, *36*, e124. [\[CrossRef\]](#) [\[PubMed\]](#)
27. Pan, L.; Hu, Y.; Ding, T.; Xie, C.; Wang, Z.; Chen, Z.; Yang, J.; Zhang, C. Aptamer-based regulation of transcription circuits. *Chem. Commun.* **2019**, *55*, 7378–7381. [\[CrossRef\]](#) [\[PubMed\]](#)
28. Etzel, M.; Mörl, M. Synthetic riboswitches: From plug and pray toward plug and play. *Biochemistry* **2017**, *56*, 1181–1198. [\[CrossRef\]](#) [\[PubMed\]](#)
29. Ogawa, A.; Maeda, M. An artificial aptazyme-based riboswitch and its cascading system in E. coli. *ChemBioChem* **2008**, *9*, 206–209. [\[CrossRef\]](#) [\[PubMed\]](#)
30. Chappell, J.; Takahashi, M.K.; Lucks, J.B. Creating small transcription activating RNAs. *Nat. Chem. Biol.* **2015**, *11*, 214–220. [\[CrossRef\]](#)
31. Green, A.A.; Silver, P.A.; Collins, J.J.; Yin, P. Toehold switches: De-novo-designed regulators of gene expression. *Cell* **2014**, *159*, 925–939. [\[CrossRef\]](#) [\[PubMed\]](#)
32. Stanton, B.C.; Nielsen, A.A.; Tamsir, A.; Clancy, K.; Peterson, T.; Voigt, C.A. Genomic mining of prokaryotic repressors for orthogonal logic gates. *Nat. Chem. Biol.* **2014**, *10*, 99–105. [\[CrossRef\]](#)
33. Chappell, J.; Westbrook, A.; Verosloff, M.; Lucks, J.B. Computational design of small transcription activating RNAs for versatile and dynamic gene regulation. *Nat. Commun.* **2017**, *8*, 1051. [\[CrossRef\]](#)
34. Verosloff, M.; Chappell, J.; Perry, K.L.; Thompson, J.R.; Lucks, J.B. PLANT-Dx: A molecular diagnostic for point-of-use detection of plant pathogens. *ACS Synth. Biol.* **2019**, *8*, 902–905. [\[CrossRef\]](#)
35. Glasscock, C.J.; Biggs, B.W.; Lazar, J.T.; Arnold, J.H.; Burdette, L.A.; Valdes, A.; Kang, M.-K.; Tullman-Ercek, D.; Tyo, K.E.; Lucks, J.B. Dynamic Control of Gene Expression with Riboregulated Switchable Feedback Promoters. *ACS Synth. Biol.* **2021**. [\[CrossRef\]](#)
36. Green, A.A.; Kim, J.; Ma, D.; Silver, P.A.; Collins, J.J.; Yin, P. Complex cellular logic computation using ribocomputing devices. *Nature* **2017**, *548*, 117–121. [\[CrossRef\]](#) [\[PubMed\]](#)
37. Callura, J.M.; Dwyer, D.J.; Isaacs, F.J.; Cantor, C.R.; Collins, J.J. Tracking, tuning, and terminating microbial physiology using synthetic riboregulators. *Proc. Natl. Acad. Sci. USA* **2010**, *107*, 15898–15903. [\[CrossRef\]](#) [\[PubMed\]](#)
38. Lehr, F.-X.; Hanst, M.; Vogel, M.; Kremer, J.; Göringer, H.U.; Suess, B.; Koepl, H. Cell-free prototyping of AND-logic gates based on heterogeneous RNA activators. *ACS Synth. Biol.* **2019**, *8*, 2163–2173. [\[CrossRef\]](#)
39. Bartoli, V.; Meaker, G.A.; Di Bernardo, M.; Gorochofski, T.E. Tunable genetic devices through simultaneous control of transcription and translation. *Nat. Commun.* **2020**, *11*, 2095. [\[CrossRef\]](#) [\[PubMed\]](#)
40. Greco, F.V.; Pandi, A.; Erb, T.J.; Grierson, C.S.; Gorochofski, T.E. Harnessing the central dogma for stringent multi-level control of gene expression. *Nat. Commun.* **2021**, *12*, 1738. [\[CrossRef\]](#)
41. Lee, Y.J.; Kim, S.-J.; Moon, T.S. Multilevel regulation of bacterial gene expression with the combined STAR and antisense RNA system. *ACS Synth. Biol.* **2018**, *7*, 853–865. [\[CrossRef\]](#) [\[PubMed\]](#)
42. Westbrook, A.M.; Lucks, J.B. Achieving large dynamic range control of gene expression with a compact RNA transcription-translation regulator. *Nucleic Acids Res.* **2017**, *45*, 5614–5624. [\[CrossRef\]](#) [\[PubMed\]](#)
43. Chen, Y.-J.; Liu, P.; Nielsen, A.A.; Brophy, J.A.; Clancy, K.; Peterson, T.; Voigt, C.A. Characterization of 582 natural and synthetic terminators and quantification of their design constraints. *Nat. Methods* **2013**, *10*, 659–664. [\[CrossRef\]](#) [\[PubMed\]](#)
44. Lee, Y.J.; Moon, T.S. Design rules of synthetic non-coding RNAs in bacteria. *Methods* **2018**, *143*, 58–69. [\[CrossRef\]](#) [\[PubMed\]](#)
45. Larson, M.H.; Greenleaf, W.J.; Landick, R.; Block, S.M. Applied force reveals mechanistic and energetic details of transcription termination. *Cell* **2008**, *132*, 971–982. [\[CrossRef\]](#) [\[PubMed\]](#)
46. Cambray, G.; Guimaraes, J.C.; Mutalik, V.K.; Lam, C.; Mai, Q.-A.; Thimmaiah, T.; Carothers, J.M.; Arkin, A.P.; Endy, D. Measurement and modeling of intrinsic transcription terminators. *Nucleic Acids Res.* **2013**, *41*, 5139–5148. [\[CrossRef\]](#) [\[PubMed\]](#)
47. McDowell, J.C.; Roberts, J.W.; Jin, D.J.; Gross, C. Determination of intrinsic transcription termination efficiency by RNA polymerase elongation rate. *Science* **1994**, *266*, 822–825. [\[CrossRef\]](#)
48. iGEM Parts. Terminators/Catalog. Available online: <http://parts.igem.org/Terminators/Catalog> (accessed on 29 April 2021).
49. Wandera, K.G.; Collins, S.P.; Wimmer, F.; Marshall, R.; Noireaux, V.; Beisel, C.L. An enhanced assay to characterize anti-CRISPR proteins using a cell-free transcription-translation system. *Methods* **2020**, *172*, 42–50. [\[CrossRef\]](#)



- 
50. Yeung, E.; Ng, A.; Kim, J.; Sun, Z.Z.; Murray, R.M. Modeling the effects of compositional context on promoter activity in an *E. coli* extract based transcription-translation system. In Proceedings of the 53rd IEEE Conference on Decision and Control, Los Angeles, CA, USA, 15–17 December 2014; pp. 5405–5412.
  51. Shin, J.; Noireaux, V. Efficient cell-free expression with the endogenous *E. Coli* RNA polymerase and sigma factor 70. *J. Biol. Eng.* **2010**, *4*, 8. [[CrossRef](#)]
  52. Kamionka, A.; Bogdanska-Urbaniak, J.; Scholz, O.; Hillen, W. Two mutations in the tetracycline repressor change the inducer anhydrotetracycline to a corepressor. *Nucleic Acids Res.* **2004**, *32*, 842–847. [[CrossRef](#)] [[PubMed](#)]
  53. Dragosits, M.; Nicklas, D.; Tagkopoulos, I. A synthetic biology approach to self-regulatory recombinant protein production in *Escherichia coli*. *J. Biol. Eng.* **2012**, *6*, 2. [[CrossRef](#)]
  54. Lim, H.G.; Kwak, D.H.; Park, S.; Woo, S.; Yang, J.-S.; Kang, C.W.; Kim, B.; Noh, M.H.; Seo, S.W.; Jung, G.Y. *Vibrio* sp. dhg as a platform for the biorefinery of brown macroalgae. *Nat. Commun.* **2019**, *10*, 2486. [[CrossRef](#)] [[PubMed](#)]
  55. Jeong, D.; Klocke, M.; Agarwal, S.; Kim, J.; Choi, S.; Franco, E.; Kim, J. Cell-free synthetic biology platform for engineering synthetic biological circuits and systems. *Methods Protoc.* **2019**, *2*, 39. [[CrossRef](#)] [[PubMed](#)]
  56. Weaver, K.E.; Chen, Y.; Miiller, E.M.; Johnson, J.N.; Dangler, A.A.; Manias, D.A.; Clem, A.M.; Schjodt, D.J.; Dunny, G.M. Examination of *Enterococcus faecalis* toxin-antitoxin system toxin Fst function utilizing a pheromone-inducible expression vector with tight repression and broad dynamic range. *J. Bacteriol.* **2017**, *199*, e00065-17. [[CrossRef](#)] [[PubMed](#)]
  57. Lee, J.W.; Chan, C.T.; Slomovic, S.; Collins, J.J. Next-generation biocontainment systems for engineered organisms. *Nat. Chem. Biol.* **2018**, *14*, 530–537. [[CrossRef](#)] [[PubMed](#)]
  58. Chan, C.T.; Lee, J.W.; Cameron, D.E.; Bashor, C.J.; Collins, J.J. ‘Deadman’ and ‘Passcode’ microbial kill switches for bacterial containment. *Nat. Chem. Biol.* **2016**, *12*, 82–86. [[CrossRef](#)]
  59. Kushwaha, M.; Rostain, W.; Prakash, S.; Duncan, J.N.; Jaramillo, A. Using RNA as molecular code for programming cellular function. *ACS Synth. Biol.* **2016**, *5*, 795–809. [[CrossRef](#)]